8-10-2018

Genetic Architecture of Gene Expression Traits Across Diverse Populations

Lauren S. Mogil
Loyola University Chicago, lmogil@luc.edu

Angela Andaleon
Loyola University Chicago, aandaleon@luc.edu

Alexa Badalamenti
Loyola University Chicago

Scott P. Dickinson

Xiuqing Guo

See next page for additional authors

Recommended Citation

Authors

Lauren S. Mogil, Angela Andaleon, Alexa Badalamenti, Scott P. Dickinson, Xiuqing Guo, Jerome I. Rotter, W. C. Johnson, Hae Kyung Im, Yongmei Liu, and Heather E. Wheeler
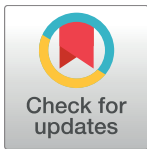
RESEARCH ARTICLE

Genetic architecture of gene expression traits across diverse populations

Lauren S. Mogil[1], Angela Andaleon[1,2], Alexa Badalamenti[2], Scott P. Dickinson[3], Xiuqing Guo[4], Jerome I. Rotter[4], W. Craig Johnson[5], Hae Kyung Im[3], Yongmei Liu[6], Heather E. Wheeler[1,2,7,8]*

1 Department of Biology, Loyola University Chicago, Chicago, Illinois, United States of America, 2 Program in Bioinformatics, Loyola University Chicago, Chicago, Illinois, United States of America, 3 Section of Genetic Medicine, Department of Medicine, University of Chicago, Chicago, Illinois, United States of America, 4 Institute for Translational Genomics and Population Sciences, Los Angeles Biomedical Research Institute and Department of Pediatrics at Harbor-UCLA Medical Center, Torrance, California, United States of America, 5 Department of Biostatistics, University of Washington, Seattle, Washington, United States of America, 6 Department of Epidemiology & Prevention, Wake Forest School of Medicine, Winston-Salem, North Carolina, United States of America, 7 Department of Computer Science, Loyola University Chicago, Chicago, Illinois, United States of America, 8 Department of Public Health Sciences, Stritch School of Medicine, Loyola University Chicago, Maywood, Illinois, United States of America

* hwheeler1@luc.edu

Abstract

For many complex traits, gene regulation is likely to play a crucial mechanistic role. How the genetic architectures of complex traits vary between populations and subsequent effects on genetic prediction are not well understood, in part due to the historical paucity of GWAS in populations of non-European ancestry. We used data from the MESA (Multi-Ethnic Study of Atherosclerosis) cohort to characterize the genetic architecture of gene expression within and between diverse populations. Genotype and monocyte gene expression were available in individuals with African American (AFA, n = 233), Hispanic (HIS, n = 352), and European (CAU, n = 578) ancestry. We performed expression quantitative trait loci (eQTL) mapping in each population and show genetic correlation of gene expression depends on shared ancestry proportions. Using elastic net modeling with cross validation to optimize genotypic predictors of gene expression in each population, we show the genetic architecture of gene expression for most predictable genes is sparse. We found the best predicted gene in each population, *TACSTD2* in AFA and *CHURC1* in CAU and HIS, had similar prediction performance across populations with $R^2 > 0.8$ in each population. However, we identified a subset of genes that are well-predicted in one population, but poorly predicted in another. We show these differences in predictive performance are due to allele frequency differences between populations. Using genotype weights trained in MESA to predict gene expression in independent populations showed that a training set with ancestry similar to the test set is better at predicting gene expression in test populations, demonstrating an urgent need for diverse population sampling in genomics. Our predictive models and performance statistics in diverse cohorts are made publicly available for use in transcriptome mapping methods at https://github.com/WheelerLab/DivPop.

Author summary

Most genome-wide association studies (GWAS) have been conducted in populations of European ancestry leading to a disparity in understanding the genetics of complex traits between populations. For many complex traits, gene regulation is critical, given the consistent enrichment of regulatory variants among trait-associated variants. However, it is still unknown how the effects of these key variants differ across populations. We used data from MESA to study the underlying genetic architecture of gene expression by optimizing gene expression prediction within and across diverse populations. The populations with genotype and gene expression data available are from individuals with African American (AFA, n = 233), Hispanic (HIS, n = 352), and European (CAU, n = 578) ancestry. After calculating the prediction performance, we found that many genes that were well predicted in one population are poorly predicted in another. We further show that a training set with ancestry similar to the test set resulted in better gene expression predictions, demonstrating the need to incorporate diverse populations in genomic studies. Our gene expression prediction models and performance statistics are publicly available to facilitate future transcriptome mapping studies in diverse populations.

Introduction

For over a decade, genome-wide association studies (GWAS) have facilitated the discovery of thousands of genetic variants associated with complex traits and new insights into the biology of these traits [1]. Most of these studies involved individuals of primarily European descent, which can lead to disparities when attempting to apply this information across populations [2–4]. Continued increases in GWAS sample sizes and new integrative methods will lead to more clinically relevant and applicable results. A recent study shows that the lack of diversity in large GWAS skew the prediction accuracy across non-European populations [5]. This discrepancy in predictive accuracy demonstrates that adding ethnically diverse populations is critical for the success of precision medicine, genetic research, and understanding the biology behind genetic variation [5–8].

Gene regulation is likely to play a critical role for many complex traits as trait-associated variants are enriched in regulatory, not protein-coding, regions [9–13]. Numerous expression quantitative trait loci (eQTLs) studies have provided insight into how genetic variation affects gene expression [14–17]. While eQTLs can act at a great distance, or in *trans*, the largest effect sizes are consistently found near the transcription start sites of genes [14–17]. Because gene expression shows a more sparse genetic architecture than many other complex traits, gene expression is amenable to genetic prediction with relatively modest sample sizes [18, 19]. This has led to new mechanistic methods for gene mapping that integrate transcriptome prediction, including PrediXcan [20] and TWAS [21]. These methods have provided useful tools for understanding the genetics of complex traits; however, most of the models have been built using predominantly European populations.

How the key variants involved in gene regulation differ among populations has not been fully explored. While the vast majority of eQTL mapping studies have been performed in populations of European descent, increasing numbers of transcriptome studies in non-European populations make the necessary comparisons between populations feasible [14, 22, 23]. An eQTL study across eight diverse HapMap populations (∼100 individuals/population) showed that the directions of effect sizes were usually consistent when an eQTL was present in two populations [14]. However, the impact of a particular genetic variant on population gene

expression differentiation is also dependent on allele frequencies, which often vary between populations. A better understanding of the degree of transferability of gene expression prediction models across populations is essential for broad application of methods like PrediXcan in the study of the genetic architecture of complex diseases and traits in diverse populations.

Here, in order to better define the genetic architecture of gene expression across populations, we combine genotype [24] and monocyte gene expression [25] data from the Multi-Ethnic Study of Atherosclerosis (MESA) for the first time. We perform eQTL mapping and optimize multi-SNP predictors of gene expression in three diverse populations. The MESA populations studied herein comprise 233 African American (AFA), 352 Hispanic (HIS), and 578 European (CAU) self-reported ancestry individuals. Using elastic net regularization and Bayesian sparse linear mixed modeling, we show sparse models outperform polygenic models in each population. We show the genetic correlation of SNP effects and the predictive performance correlation is highest between populations with the most overlapping admixture proportions. We found a subset of genes that are well predicted in the AFA and/or HIS cohorts that are poorly predicted, if predicted at all, in the CAU cohort. We also test our predictive models trained in MESA cohorts in independent cohorts from the HapMap Project [14], Geuvadis Consortium [26], and Framingham Heart Study [18, 27] and show the correlation between predicted and observed gene expression is highest when the ancestry of the test set is similar to that of the training set. By diversifying our model-building populations, new genes may be implicated in complex trait mapping studies that were not previously interrogated. Models built here have been added to PredictDB for use in PrediXcan [20] and other studies, links at https://github.com/WheelerLab/DivPop.

Results

eQTL discovery in MESA and replication in independent populations reflects ancestry and sample size

We surveyed each MESA population (AFA, HIS, CAU) and two combined populations (AFHI, ALL) for cis-eQTLs. SNPs within 1Mb of each of 10,143 genes were tested for association with monocyte gene expression levels using a linear additive model. The MESA HIS cohort includes many individuals with recent African admixture (S1 Fig). We compared models that included a range of genotypic principal components (0, 3, 5, 10) and PEER factors (0, 10, 20, 30) to adjust for hidden confounders in the expression data [28]. Genotypic principal components (PCs) and PEER factors were computed within each population prior to cis-eQTL mapping. While 3 genotypic PCs controlled for inflation due to population stratification compared to 0 PCs, especially in HIS, the cis-eQTLs discovered with 3, 5, or 10 PCs were nearly the same (S2 Fig).

We calculated the true positive rates (π_1) of top cis-eQTLs (FDR < 0.05) from our MESA discovery cohorts by examining their P value distributions in several replication cohorts: Framingham Heart Study (FHS, n = 4838 European ancestry individuals, whole blood expression microarray) [27], Geuvadis (GEU, n = 344 European and 77 African ancestry individuals, lymphoblastoid cell line (LCL) RNA-Seq) [26], Yoruba from Ibadan, Nigeria (YRI, n = 107, LCL expression microarray) [14], and Mexican ancestry from Los Angeles (MXL, n = 45, LCL expression microarray) [14]. True positive rates were similar across PEER factors except for models with 0 PEER factors, which were either higher or lower depending on the replication population (Fig 1). Because the FHS replication population is the largest, true positive rates were higher across discovery populations. True positive rates for eQTLs discovered in AFA were higher compared to the other MESA populations in replication populations that include African ancestry individuals (GEU and YRI). eQTLs discovered in AFA and HIS yielded
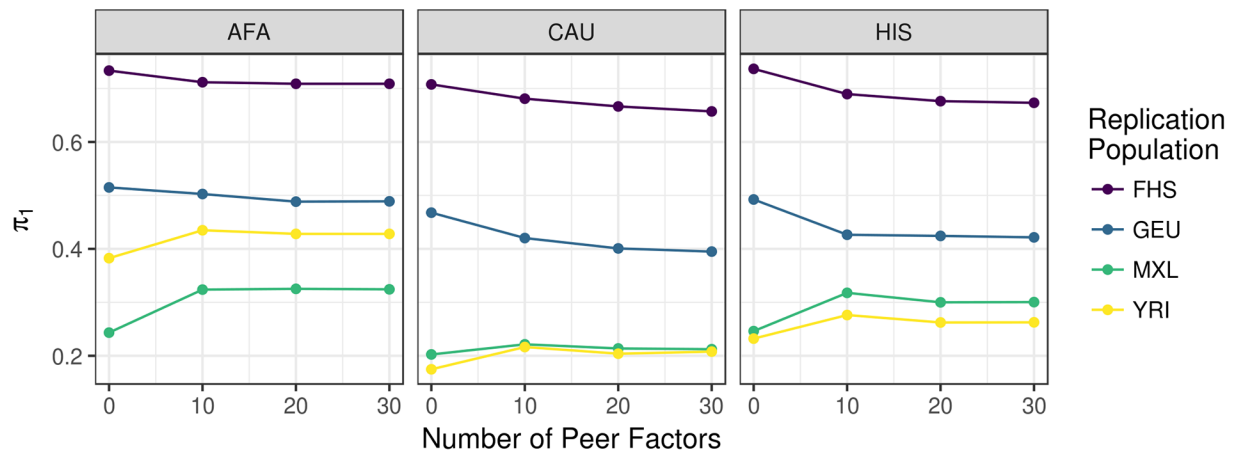
Fig 1. Summary of eQTL analyses in MESA populations. True positive rate π_1 statistics [29] for cis-eQTLs are plotted vs. the number of PEER factors used to adjust for hidden confounders in the expression data of both discovery and replication populations. The MESA discovery population is listed in the gray title box and the color of the each line represents each replication population. Higher π_1 values indicate a stronger replication signal. π_1 is calculated when the SNP-gene pair from the discovery population is present in the replication population. All models shown included 3 genotypic principal components. AFA = MESA African American, CAU = MESA European American, HIS = MESA Hispanic American, FHS = Framingham Heart Study, GEU = Geuvadis, MXL = Mexicans in Los Angeles, YRI = Yoruba in Ibadan, Nigeria.

https://doi.org/10.1371/journal.pgen.1007586.g001

higher true positive rates in both YRI and MXL compared to eQTLs discovered in CAU (Fig 1). A full pairwise comparison of π_1 statistics across all discovery and replication population PEER factor combinations showed similar trends (S3 Fig).

As expected, the sample size of the discovery population influences the number of eQTLs mapped (Table 1). Hundreds of thousands to millions of SNPs were found to associate with gene expression (eSNPs) and most genes had at least one associated variant (eGenes) at FDR < 0.05, with the absolute numbers correlating with sample size (Table 1). Cis-eQTL summary statistics for each population are available at https://github.com/WheelerLab/DivPop.

Genetic effect size correlations between populations reflect shared ancestry proportions

We estimated the local (cis-region SNPs) heritability (h^2) for each gene and the genetic correlation (rG) between genes in each MESA population. We used the average information-REML algorithm implemented in GCTA [30, 31] to estimate rG, which is constrained between -1 and 1 for each gene (See Methods). As in Brown et al. [32], the sample sizes for gene expression

Table 1. cis-eQTL (FDR < 0.05) counts across MESA populations.

Population	number eSNPs	number eGenes
AFA (n = 233)	412,450	6837
HIS (n = 352)	890,100	7974
CAU (n = 578)	1,290,814	7925
AFHI (n = 585)	1,126,620	8628
ALL (n = 1163)	1,652,365	8877

Linear additive models were adjusted for 3 genotypic principal components and 10 PEER factors. FDR = Benjamini-Hochberg false discovery rate. AFA = African American, HIS = Hispanic American, CAU = European American, AFHI = AFA and HIS, ALL = AFA, HIS, and CAU.

https://doi.org/10.1371/journal.pgen.1007586.t001

Table 2. Genetic correlation (rG) between MESA populations.

pop pair	mean rG	SE rG	genes that converged
AFA-CAU	0.46	0.0080	9209
AFA-HIS	0.57	0.0076	9313
HIS-CAU	0.62	0.0072	9490

rG was estimated using a bivariate restricted maximum likelihood (REML) model implemented in GCTA.

https://doi.org/10.1371/journal.pgen.1007586.t002

data are too small for obtaining accurate point estimates of rG for each gene. However, the large number of genes allow us to obtain accurate estimation of the global mean rG between populations. The population pair with the highest mean rG was CAU and HIS, followed by AFA and HIS, and the least correlated pair was AFA and CAU (Table 2). Genes with larger h^2 estimates in at least one population tended to have larger rG estimates with lower standard errors (Fig 2A, S4 Fig). As the h^2 threshold for inclusion increases, the mean rG between populations also increases (Fig 2B). The same pattern is observed when the h^2 estimates are normalized by the number of SNPs in the gene (S4 Fig).

To verify that our rG analysis did not contain any small sample-size biases, we simulated gene expression phenotypes in each population with the same local h^2 distributions as the real data. For ten sets of simulated gene expression phenotypes, we estimated rG between populations and compared the simulated results to the observed results. While the mean rG ranged from 0.46-0.62 in the observed data, the mean rG in the simulated data was near zero with similar numbers of genes at -1 and 1 (Fig 2C).

Models with a sparse component outperform polygenic models for gene expression

We examined the prediction performance of a range of models using elastic net regularization [33] to characterize the genetic architecture of gene expression in each population. The mixing parameter (α) of elastic net ranges from 0-1. Models with α near 0 assume a more polygenic architecture and models with α near 1 assume a more sparse architecture. We used nested cross-validation to compute the coefficient of determination R^2 as our measure of model performance across three mixing parameters (α = 0.05, 0.5, 1). The model with α = 1 is equivalent to least absolute shrinkage and selection operator (lasso) regression [34]. When we compared the R^2 values for each gene between models, more genes had a higher R^2 with the lasso model (α = 1) than the most polygenic model tested (α = 0.05) in each population (Table 3, Fig 3). The lasso model performed similarly to the mixture model (α = 0.5), indicating elastic net is somewhat robust to α choice as long as a sparse component is included (Table 3, Fig 3).

In addition to elastic net, we used Bayesian Sparse Linear Mixed Modeling (BSLMM) [35] to estimate if the local genetic contribution to gene expression is more polygenic or sparse. This approach models the genetic contribution of the trait as the sum of a sparse component and a polygenic component. BSLMM estimates the total percent variance explained (PVE) and the parameter PGE, which represents the proportion of the genetic variance explained by sparse effects. We found that for highly heritable genes (high PVE), the sparse component (PGE) is large; however, for genes with low PVE, we are unable to determine whether the sparse or polygenic component is predominant (S5 Fig). We also estimated heritability (h^2) using a linear mixed model (LMM) [30] and Bayesian variable selection regression (BVSR) [36], which assume a polygenic and sparse architecture, respectively. It has previously been shown that BVSR performs similarly to BSLMM when the simulated architecture is sparse,
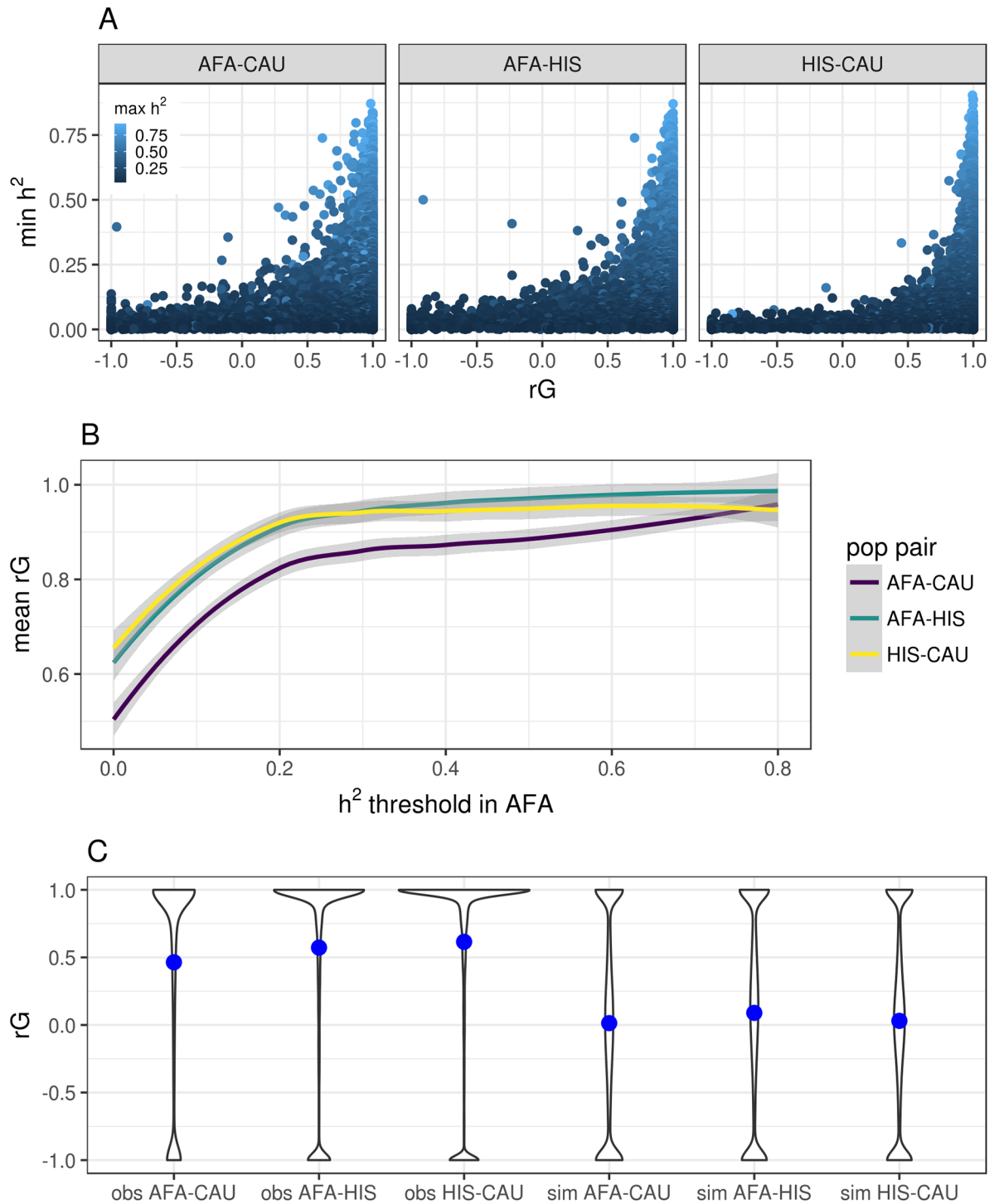
Fig 2. Genetic correlation (rG) of gene expression between MESA populations. (A) Pairwise population comparison of heritability (h^2) and rG for each gene. The y-axis is the minimum h^2, the x-axis is the genetic correlation, and the points are colored according to the maximum h^2 between the populations titling each plot. (B) Comparison of the genetic correlation between pairwise MESA populations and the subset of genes with h^2 greater than a given threshold in the AFA population. (C) Violin plots of the observed results (obs) compared to simulated expression data (sim) with the same h^2 distributions. The blue points represent the mean rG across genes for the population pair. The most correlated populations are CAU and HIS and the least correlated populations are AFA and CAU. Note more genes have an rG estimate equal to 1 in the observed data compared to the simulated data.

https://doi.org/10.1371/journal.pgen.1007586.g002

Table 3. Proportion of genes with greater lasso ($\alpha = 1$) model predictive performance (R^2) compared to elastic net models with different mixing parameter (α) values.

Population	elastic net ($\alpha = 0.05$)	elastic net ($\alpha = 0.5$)
AFA	1497/2517 (0.595)	1342/2567 (0.523)
CAU	2213/3858 (0.574)	1943/3867 (0.502)
HIS	1950/3529 (0.553)	1763/3529 (0.500)

https://doi.org/10.1371/journal.pgen.1007586.t003

but BVSR performs poorly compared to BSLMM when the simulated architecture includes a polygenic component [35]. BSLMM outperforms both LMM and BVSR in each population (S5 Fig). However, BSLMM and BVSR show greater correlation, providing further support that the sparse component dominates in the MESA cohorts (S5 Fig).
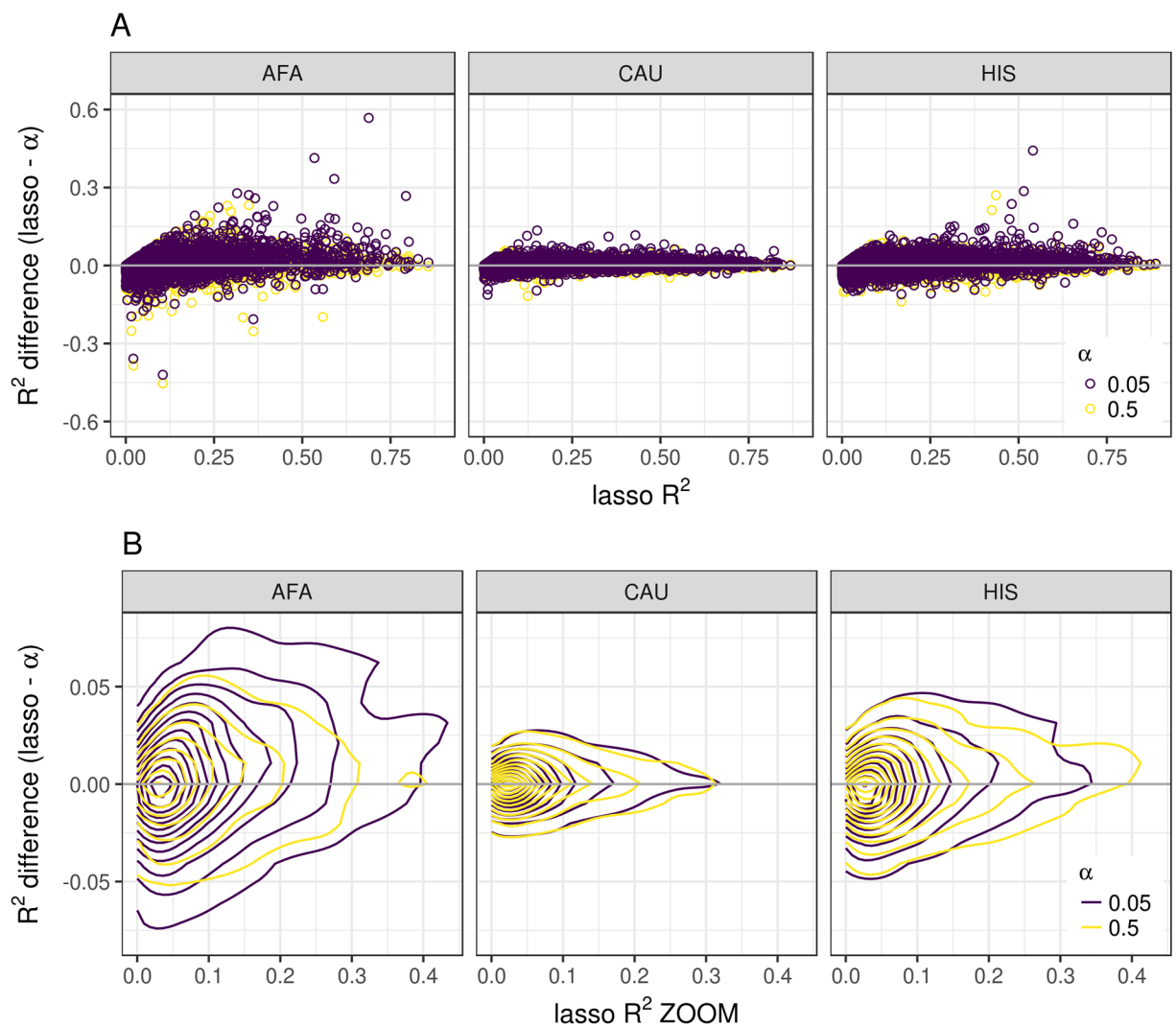
Fig 3. MESA gene expression predictive performance across a range of elastic net mixing parameters. (A) The difference between cross-validated R^2 of lasso and elastic net with mixing parameters 0.05 or 0.5 is compared to the lasso R^2 across genes in MESA populations AFA, HIS, and CAU. (B) Zoomed in plot of A using contour lines from two-dimensional kernel density estimation to visualize where the points are concentrated. The R^2 difference values (y-axis) with a mixing parameter $\alpha = 0.5$ are closer to zero indicating that they perform similarly to the lasso model. The values with a mixing parameter $\alpha = 0.05$ are above zero indicating that they perform worse than the lasso model.

https://doi.org/10.1371/journal.pgen.1007586.g003

Differences in predictive performance are due to allele frequency differences between populations

We then compared each population's gene expression predictive performance as measured by cross-validated coefficient of determination (R^2). We first fit elastic net models ($\alpha = 0.5$) using 3 genotypic PCs and gene expression levels adjusted by 0, 10, 20 or 30 PEER factors in each population. Predictive performance was higher when we used 10 PEER factors compared to no PEER factor adjustment (S6 Fig). Seeing little difference between models with 10 or more PEER factors within populations (S6 Fig), we compared predictive performance between populations using the elastic net models with 10 PEER factors. The Spearman correlation (ρ) between CAU and HIS model performance is highest ($\rho = 0.778$), followed by AFA and HIS ($\rho = 0.663$). The lowest correlation between two populations was AFA and CAU with $\rho = 0.586$ (Fig 4A). These correlation relationships mirror the European and African admixture proportions in the MESA HIS and AFA cohorts (S1 Fig).
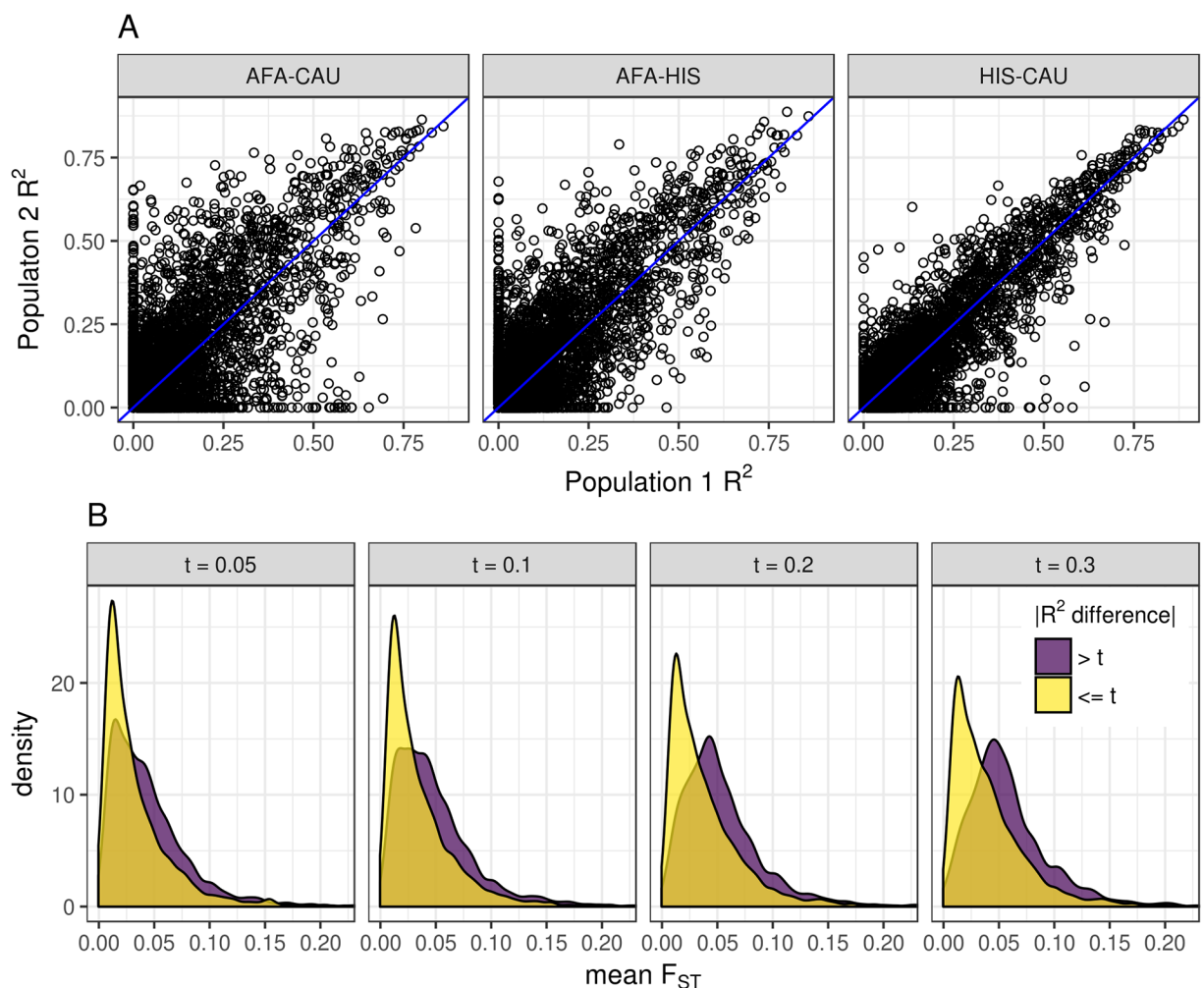
Fig 4. Allele frequency differences lead to gene expression predictive performance differences between populations. (A) Comparison of predictive performance for each gene (R^2) between each pair of populations. Predictive performance (R^2) was measured within each population using nested cross-validation. In each gray title box, population 1 is listed first and population 2 is listed second. The identity line is shown in blue. The pairwise Spearman correlations (ρ) between genes are AFA-CAU: $\rho = 0.59$, AFA-HIS: $\rho = 0.66$, HIS-CAU: $\rho = 0.78$. (B) Comparison of mean F_{ST} between gene models with large ($> t$) and small ($<= t$) differences in predictive performance R^2. Mean F_{ST} of SNPs in each gene expression prediction model between all pairwise populations was calculated. The gene groups with the larger absolute value R^2 difference between populations had significantly larger mean F_{ST} at each difference threshold, t (Wilcoxon rank sum tests, $P < 2.2 \times 10^{-16}$).

https://doi.org/10.1371/journal.pgen.1007586.g004

Because the sample sizes between MESA populations differed (Table 1), we randomly selected 233 individuals from CAU and HIS and fit elastic net models with these downsampled populations to match the AFA sample size. Predictive performance R^2 is highly correlated between the full and downsampled populations ($\rho > 0.8$). A handful of genes are better predicted with the full sample size (S7 Fig). Also, the between population correlations showed the same trend when all populations had the same sample size, with CAU and HIS the most correlated, followed by AFA and HIS (S7 Fig).

There are many genes that are well predicted in both populations and poorly predicted in both populations. For example, *TACSTD2*, was well predicted across populations with an $R^2 > 0.84$ in each population. On the other hand, there are some genes that are well predicted in one population, but poorly predicted in the other and vice versa (Fig 4A).

To test the hypothesis that allele frequency differences between populations are influencing predictive power, we performed a fixation index (F_{ST}) analysis. For each population pair, we calculated the mean F_{ST} for SNPs in each gene expression prediction model. Gene models with an absolute value R^2 difference between populations greater than 0.05 had significantly higher mean F_{ST} distribution than those with a smaller difference (Wilcoxon $P = 2.7 \times 10^{-66}$). The significant increase in mean F_{ST} was robust across R^2 difference thresholds (Fig 4B). Similar significant differences were observed when the SNP F_{ST} values were weighted by elastic net model betas across R^2 difference thresholds from 0.05-0.3 (S8 Fig).

Gene expression prediction improves when training set has similar ancestry to test set

In order to further compare gene expression prediction model performance between populations, using the models built in each MESA population, we predicted gene expression in our replication populations: FHS, GEU, MXL, and YRI. We calculated the true positive rates (π_1 statistics) [29] for predicted vs. observed expression in each replication cohort when different numbers of gene models were included based on MESA predictive performance (Table 4, Fig 5). As expected, true positive rates were higher across model training populations for the largest replication population, FHS. For GEU, which includes European and African ancestry individuals, the best performing models were trained using all the MESA individuals (ALL, Fig 5). Prediction in YRI was best using AFA or AFHI models and prediction in MXL was optimal using the CAU models (Fig 5). These results demonstrate that when comparing predicted expression levels to the observed, a balance of the training population with ancestry most similar to the test population and total sample size leads to optimal predicted gene expression.

Table 4. Number of genes with models at different R^2 thresholds.

Model	$R^2 \geq 0$	$R^2 \geq 0.01$	$R^2 \geq 0.05$	$R^2 \geq 0.1$	$R^2 \geq 0.2$
AFA	3486	3006	2153	1584	910
HIS	4457	3879	2704	1913	1152
CAU	4901	4128	2753	1921	1149
AFHI	5778	4926	3303	2304	1308
ALL	6896	5672	3532	2407	1336

The number of genes in MESA (AFA = African American, HIS = Hispanic American, CAU = European American, AFHI = AFA and HIS, ALL = AFA, HIS, and CAU) training sets that predict gene expression

https://doi.org/10.1371/journal.pgen.1007586.t004
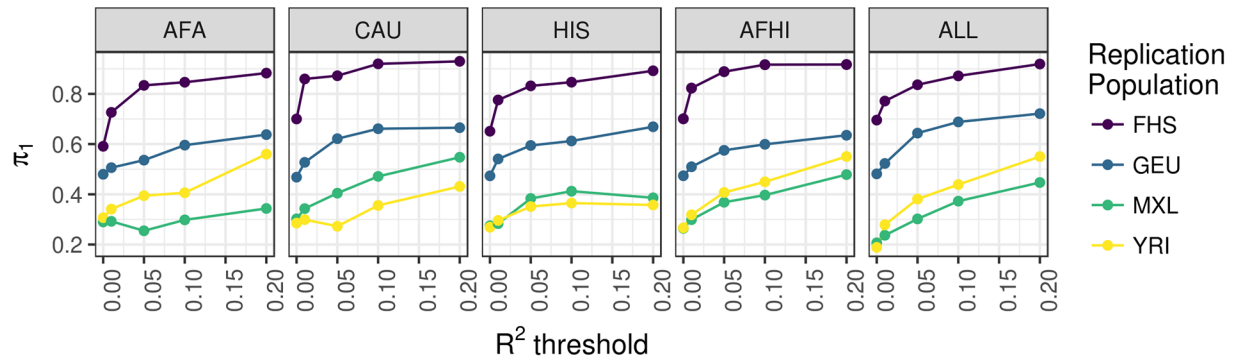
Fig 5. Predictive performance in independent test cohorts across MESA population models. True positive rate π_1 statistics [29] for replication cohort prediction are plotted vs. the training population model predictive performance R^2. The MESA training population is listed in the gray title box and the color of each line represents each replication population. Higher π_1 values indicate a higher true positive rate of predicted expression in the replication cohort using the MESA model vs. observed expression in the replication cohort. All models shown included 3 genotypic principal components and 10 PEER factors. AFA = MESA African American, CAU = MESA European American, HIS = MESA Hispanic American, FHS = Framingham Heart Study, GEU = Geuvadis, MXL = Mexicans in Los Angeles, YRI = Yoruba in Ibadan, Nigeria.

https://doi.org/10.1371/journal.pgen.1007586.g005

Gene-based association using multiethnic predictors

Gene-based association methods like PrediXcan, TWAS, and S-PrediXcan have been developed to use genotype data to discover genes whose predicted expression is associated with a phenotype of interest [20, 21, 37]. To date, most predicted expression models available for these methods were trained in European ancestry cohorts. We used the five MESA models with S-PrediXcan [37] and publicly available multiancestry GWAS summary statistics from a large asthma study by the Trans-National Asthma Genetic Consortium (TAGC) [38]. While all MESA models performed similarly, the top genes differed across models (Fig 6, S1 Table). Many genes identified by S-PrediXcan were not previously implicated in the TAGC GWAS [38] (Table 5, S1 Table). Two of the genes that associated with asthma using the ALL models were not predicted in CAU and thus not even tested, demonstrating the additional information non-European populations may add to studies. They include *C2* (complement C2) and *BLOC1S1* (biogenesis of lysosomal organelles complex 1 subunit 1), which are on different chromosomes. Neither gene has been implicated in asthma GWAS before, but both are associated with age-related macular degeneration, another inflammation-related disease [39]. All summary statistics from our S-PrediXcan analyses are in S2 Table.

Discussion

We compared three MESA populations (AFA, HIS, and CAU) to better understand the genetic architecture of gene expression in diverse populations. We optimized predictors of gene expression using elastic net regularization and found that models with a sparse component outperform polygenic models. Between populations, the genetic correlation of gene expression is higher when continental ancestry proportions are more similar. We identified genes that are better predicted in one population and poorly predicted in another due to allele frequency differences. We tested our predictors developed in MESA in independent cohorts and found that the best prediction of gene expression occurred when the training set included individuals with similar ancestry to the test set.

As seen in other studies [18, 21, 40], we show models with a sparse component outperform polygenic only models for gene expression prediction across populations. Thus, the genetic architecture of gene expression for many genes has a substantial sparse component. Notably,
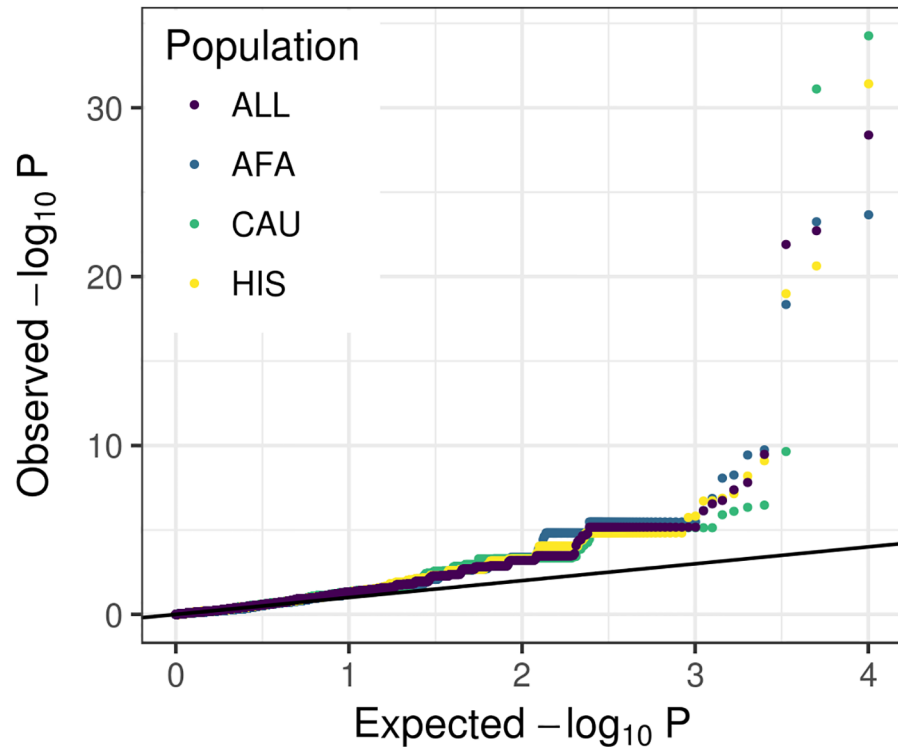
Fig 6. Comparison of S-PrediXcan results using summary statistics from a multiancestry GWAS of asthma and different prediction models. Summary statistics were retrieved from the GWAS Catalog for the Trans-National Asthma Genetic Consortium study [38]. Q-Q plots of S-PrediXcan results using gene expression prediction models built in each MESA population.

https://doi.org/10.1371/journal.pgen.1007586.g006

some genes do perform better in more polygenic models as shown here (genes below the horizontal zero line in Fig 3 and S5 Fig) and in Zeng et al. [41]. Larger sample sizes may reveal an additional polygenic component that may improve prediction for some genes. However, the population with the largest sample size (CAU) showed the least variability between models (Fig 3), suggesting that a more polygenic model does not add much to the predictive performance of a sparse model with fewer predictors. Thus, to balance these observations, we recommend using models that include a mixture of polygenic and sparse components like elastic net ($\alpha \simeq 0.5$) [33], BSLMM [35], and latent Dirichlet process regression [41].

Table 5. Summary of S-PrediXcan results using MESA models in a multiancestry GWAS of asthma [38].

Model	Bonferroni threshold	significant genes	also significant in GWAS	also significant using CAU
AFA	1.5e-5	10	4	6/10
HIS	1.1e-5	14	4	4/12
CAU	1.1e-5	17	7	NA
AFHI	9.2e-6	16	4	8/14
ALL	8.1e-6	17	5	10/15

Column 3: The number of genes using MESA gene expression prediction models (AFA = African American, HIS = Hispanic American, CAU = European American, AFHI = AFA and HIS, ALL = AFA, HIS, and CAU) that were significant after Bonferroni correction with each model; Column 4: Of the significant genes, the number of genes also implicated in the multiancestry GWAS (listed in Table 1, Table 2, or Figure 2 in [38]). Column 5: Of the significant genes, the number that were also significant using the S-PrediXcan CAU model out of the number tested in CAU.

https://doi.org/10.1371/journal.pgen.1007586.t005

We estimated the genetic correlation between each population pair for each gene. Populations with more shared ancestry as defined by clustering of genotypic principal components showed higher mean correlation across genes (S1 Fig, Table 2). As estimated heritability of genes increase, the mean genetic correlation between populations also increases (Fig 2B), which indicates the genetic architecture underlying gene expression is similar for the most heritable genes. However, even though prediction across populations is possible for some of the most heritable genes, we define a class of genes where predictive performance drops substantially between populations. We show this drop is due to allele frequency differences (larger F_{ST}) between populations.

We tested our predictive gene expression models built in the MESA populations in several replication populations. As expected, the YRI gene expression prediction was best when using the AFA, AFHI, or ALL training sets, which each include individuals with African-ancestry admixture (Fig 5). The best gene expression prediction for MXL was with the CAU training set, which may reflect the lack of recent African ancestry in MXL [6] compared to the MESA HIS population (S1 Fig). For GEU, the best MESA prediction population was ALL, which indicates that multi-ethnic cohorts like GEU benefit from a pooled training set containing individuals of diverse ancestries. Thus, it may be beneficial to build gene expression models using training populations with a similar allele frequency spectrum to that of the test cohort taking into account SNPs that are interrogated in both populations. A similar cohort-specific strategy was used to increase power to detect genes associated with warfarin dose using PrediXcan in African Americans [42].

We applied S-PrediXcan using our MESA models to summary statistics from a multiancestry GWAS of asthma [38]. We found several novel and previously reported genes significantly associated with asthma (Table 5, S1 Table). Of the genes not implicated in the Demenais et al. GWAS [38], most were associated with inflammation-related diseases in the GWAS Catalog [1]. We found increased predicted *ADORA1* expression significantly associated with increased asthma risk in 4/5 MESA models tested (S2 Table). While *ADORA1* was not significant in Demenais et. al. [38], the gene has previously been reported to associate with asthma in a study investigating the relationships between phenotypes, which also found that immune-related disease associations cluster together [43]. Similar inflammation mechanisms could explain why two genes (*C2* and *BLOC1S1*) previously associated with age-related macular degeneration [39] might also be implicated in asthma as shown here.

Predictive models of gene expression developed in this study and performance statistics are made publicly available at https://github.com/WheelerLab/DivPop for use in future studies of complex trait genetics across diverse populations. As in our S-PrediXcan analysis of asthma, multiancestry transcriptome integration may reveal new genes not implicated in European only studies. Inclusion of diverse populations in complex trait genetics is crucial for equitable implementation of precision medicine.

Materials and methods

Ethics statement

This work was approved by the Loyola University Chicago Institutional Review Board (Project numbers 2014 and 2310). All data were previous collected and analyzed anonymously.

Genomic and transcriptomic training data

The Multi-Ethnic Study of Atherosclerosis (MESA). MESA includes 6814 individuals consisting of 53% females and 47% males between the ages of 45-84 [24]. The individuals were recruited from 6 sites across the US (Baltimore, MD; Chicago, IL; Forsyth County, NC; Los

Angeles County, CA; northern Manhattan, NY; St.Paul, MN). MESA cohort population demographics were 39% European American (CAU), 22% Hispanic American (HIS), 28% African American (AFA), and 12% Chinese American (CHN). Of those individuals, RNA was collected from CD14+ monocytes from 1264 individuals across three populations (AFA, HIS, CAU) and quantified on the Illumina Ref-8 BeadChip [25]. Individuals with both genotype (dbGaP: phs000209.v13.p3) and expression data (GEO: GSE56045) included 234 AFA, 386 HIS, and 582 CAU. Illumina IDs were converted to Ensembl IDs using the RefSeq IDs from MESA and gencode.v18 (gtf and metadata files) to match Illumina IDs to Ensembl IDs. If there were multiple Illumina IDs corresponding to an Ensembl ID, the average of those values was used as the expression level.

Genomic and transcriptomic test data

Stranger et al. HapMap data. We obtained lymphoblastoid cell line (LCL) microarray transcriptome data from Stranger et al. [14] for HapMap populations of interest, including 45 Mexican ancestry individuals in Los Angeles, CA, USA (MXL) and 107 Yoruba individuals in Ibadan, Nigeria (YRI) (Illumina Sentrix Human-6 Expression BeadChip version 2, Array Express: E-MTAB-264). We obtained genotype data from the 1000 Genomes Project (phase3 v5a 20130502) [44]. HapMap genotypes in individuals not sequenced through the 1000 Genomes Project were imputed using the Michigan Imputation Server for a total of 6-13 million SNPs per population, after undergoing quality control [45]. These imputed samples were then merged with the individuals that were previously sequenced, filtering the SNPs (imputation $R^2 > 0.8$, MAF > 0.01, HWE p $> 1e-06$).

Geuvadis Consortium (GEU). We obtained RNA sequencing transcriptome data from the Geuvadis Consortium (GEU) at https://www.ebi.ac.uk/arrayexpress/experiments/ E-GEUV-1/ and genotype data from the 1000 Genomes Project (phase3 v5a 20130502) [26, 44]. The GEU cohort includes 78 Utah residents with Northern and Western European ancestry, 89 Finnish from Finland, 85 British from England and Scotland, 92 Toscani in Italy and 77 Yoruba in Ibadan, Nigeria individuals [26].

Framingham Heart Study (FHS). We obtained genotype and exon expression array (Affymetrix Human Exon 1.0 ST microarray) data [27] through application to dbGaP accession phs000007.v29.p1. Genotype imputation and gene level quantification were performed by our group previously [18], leaving 4838 European ancestry individuals with both genotypes and observed gene expression levels for analysis.

Quality control of genomic and transcriptomic data

We imputed genotypes in the MESA populations using the Michigan Imputation Server and 1000 genomes phase 3 v5 reference panel and Eagle v2.3. Reference populations were EUR for CAU and mixed population for AFA and HIS [44–46]. The results were filtered by $R^2 < 0.8$, MAF > 0.01, and ambiguous strand SNPs were removed. This left 9,352,383 SNPs in AFA, 7,201,805 SNPs in HIS, and 5,559,636 SNPs in CAU for further analysis. Quality control and cleaning of the genotype data was done using PLINK (https://www.cog-genomics.org/plink2). SNPs were filtered by call rates less than 99%. Prior to IBD and principal component (PC) analysis, SNPs were LD pruned by removing 1 SNP in a 50 SNP window if $r^2 > 0.3$. One of a pair of related individuals (IBD > 0.05) were removed. Pruned genotypes were merged with HapMap populations and EIGENSTRAT [47] was used to perform PC analysis both across (S1 Fig) and within populations. Final sample sizes for each population post quality control are AFA = 233, HIS = 352, and CAU = 578. We used 5-7 million non-LD pruned SNPs per population post quality control. PEER factor analysis within each population was performed on the

expression data using the peer R package in order to correct for potential batch effects and experimental confounders [28].

eQTL analysis

We used Matrix eQTL [48] to perform a genome-wide cis-eQTL analysis in each population separately (AFA, HIS, CAU), in the AFA and HIS combined (AFHI), and in all three populations combined (ALL). We used SNPs with MAF > 0.01 and defined cis-acting as SNPs within 1 Mb of the transcription start site (TSS). We tested a range of linear regression models with 0, 3, 5, or 10 within population genotypic PC covariates and 0, 10, 20, or 30 within population PEER factors [28]. The false discovery rate (FDR) for each SNP was calculated using the Benjamini-Hochberg procedure. We estimate the pairwise population eQTL true positive rates with π_1 statistics using the qvalue method [17, 29]. π_1 is the expected true positive rate and was estimated by selecting the SNP-gene pairs with FDR < 0.05 in each discovery cohort (MESA) and examining their P value distribution in each replication cohort (FHS, GEU, MXL, YRI). π_0 is the proportion of false positives estimated by assuming a uniform distribution of null P values and $\pi_1 = 1 - \pi_0$ [29].

Genetic correlation analysis

We performed eQTL effect size comparisons between populations using Genome-wide Complex Trait Analysis (GCTA) software [30]. We performed a bivariate restricted maximum likelihood (REML) analysis to estimate the genetic correlation (rG) between each pair of MESA populations for each gene [31]. As in the eQTL analysis, we compared cis-region (within 1 Mb) SNPs for each gene. In our implementation, the models can be written as

$$y_1 = \mathbf{X}_1 b_1 + \mathbf{Z}_1 g_1 + e_1$$

for population 1 and

$$y_2 = \mathbf{X}_2 b_2 + \mathbf{Z}_2 g_2 + e_2$$

for population 2, where y_1 and y_2 are vectors of gene expression values, b_1 and b_2 are vectors of fixed effects, g_1 and g_2 are vectors of random polygenic effects, and e_1 and e_2 are residuals for populations 1 and 2, respectively. $\mathbf{X}$ and $\mathbf{Z}$ are incidence matrices for the effects b and g, respectively. The variance covariance matrix ($\mathbf{V}$) is defined as

$$\mathbf{V} = \begin{bmatrix} \mathbf{Z}_1 \mathbf{A} \mathbf{Z}_1' \sigma_{g1}^2 + \mathbf{I}\sigma_{e1}^2 & \mathbf{Z}_1 \mathbf{C} \mathbf{Z}_2' \sigma_{g1g2}^2 \\ \mathbf{Z}_2 \mathbf{C} \mathbf{Z}_1' \sigma_{g1g2}^2 & \mathbf{Z}_2 \mathbf{B} \mathbf{Z}_2' \sigma_{g2}^2 + \mathbf{I}\sigma_{e2}^2 \end{bmatrix}$$

where $\mathbf{A}$, $\mathbf{B}$, and $\mathbf{C}$ are the genetic relationship matrices based on SNP information for population 1, population 2, and both populations combined, respectively [30], $\mathbf{I}$ is an identity matrix, σ_g^2 is the genetic variance, σ_e^2 the is residual variance, and σ_{g1g2}^2 is the covariance between g_1 and g_2. In our models, the residual covariance component is ignored because no individual belongs to two populations. We used the average information-REML algorithm implemented in GCTA [31] to estimate rG, which is constrained between -1 and 1 for each gene by bending the variance-covariance matrix to be positive definite. The GCTA command per gene is: `gcta64 --grm <pop1-pop2-combined> --reml-bivar --pheno <gene-exp> --out <out-file>`.

As in Brown et al. [32], the sample sizes for gene expression data are too small for obtaining accurate point estimates of rG for each gene. However, the large number of genes allow us to obtain accurate estimation of the global mean rG between populations. To verify that our rG

analysis did not contain any small sample-size biases, we simulated gene expression pheno-types in each population with the same local heritability (h^2) distributions as the real data. Effect sizes of cis-region SNPs for each gene were randomly generated from a standard normal distribution such that the individual population h^2 estimate would be the same as the observed data. For ten sets of simulated gene expression phenotypes, we estimated rG between populations and compared the simulated results to the observed results (Fig 2).

Prediction model optimization

We used the glmnet R package [33] to fit an elastic net model to predict gene expression from cis-region SNP genotypes. The elastic net regularization penalty is controlled by the mixing parameter alpha, which can vary between ridge regression ($\alpha = 0$) and lasso ($\alpha = 1$, default). A gene with the optimal predictive performance when $\alpha = 0$ has a polygenic architecture, whereas a gene with optimal performance when $\alpha = 1$ has a sparse genetic architecture. In the MESA cohort we tested three values of the alpha mixing parameter (0.05, 0.5, and 1) and a range of PEER factors (0, 10, 20, 30) for optimal prediction of gene expression of 10,143 genes for each population alone (AFA, CAU, HIS), AFA and HIS combined (AFHI), and all three populations combined (ALL). We used the PredictDB pipeline developed by the Im lab to pre-process, train, and compile elastic net results into database files to use as weights for gene expression prediction [37]. We quantified the predictive performance of each model via nested cross-validation. We split the data into 5 disjoint folds, roughly equal in size, and for each fold, we calculated a 10-fold cross-validated elastic net model in 4/5 of the data where the lambda tuning parameter is cross-validated. Then, using predicted and observed gene expression, we calculate the coefficient of determination (R^2) for how the model predicts on the held-out fold. We report the mean R^2 over all 5 folds as our measure of model performance. R^2 is defined as

$$1 - \frac{\sum (y_o - y_p)^2}{\sum (y_o - \bar{y}_o)^2}$$

where y_o is observed expression, y_p is predicted expression, and $\bar{y}_o$ is the mean of observed expression. See https://github.com/WheelerLab/DivPop.

We used the software GEMMA [49] to implement Bayesian Sparse Linear Mixed Modeling (BSLMM) [35] for each gene with 100K sampling steps per gene. BSLMM estimates the PVE (the proportion of variance in phenotype explained by the additive genetic model, analogous to the h^2 estimated in GCTA) and PGE (the proportion of genetic variance explained by the sparse effects terms where 0 means that genetic effect is purely polygenic and 1 means that the effect is purely sparse). From the second half of the sampling iterations for each gene, we report the median and the 95% credible sets of the PVE and PGE. We also estimated heritability (h^2) using a linear mixed model (LMM) implemented in GCTA [30] and Bayesian variable selection regression (BVSR) [36], which assume a polygenic and sparse architecture, respectively. We used the software piMASS for Bayesian variable selection regression (BVSR) [36]. For each gene, we used 10,000 burn-in steps and 100,000 sampling steps in the BVSR Markov chain Monte Carlo algorithm. From the output of every 10 sampling steps, we report the median re-estimated PVE based on sampling posterior effect sizes.

Comparing prediction models between MESA populations

We calculated the fixation index (F_{ST}) [50] for each SNP between each pair of populations using PLINK. Then, for each gene expression prediction model, we calculated both the mean F_{ST} and weighted average F_{ST} for SNPs in the model. In the weighted average calculation, F_{ST}

values were multiplied by the elastic net model beta value to give SNPs with larger effect sizes more weight. We compared mean and weighted average F_{ST} values between genes with divergent predictive performance and genes with similar predictive performance between populations using Wilcoxon rank sum tests. To test for robustness across thresholds, we varied the absolute value R^2 difference threshold to define the divergent and similar groups from 0.05-0.3.

Testing prediction models in independent replication cohorts

Using our elastic net models built in MESA AFA, HIS, CAU, AFHI, and ALL ($\alpha = 0.5$ with 10 PEER factors and 3 genotypic PCs), we predicted gene expression from genotypes in independent test populations: FHS, GEU, MXL, and YRI. As for eQTLs, we estimated the pairwise population prediction true positive rates with π_1 statistics using the qvalue method [17, 29]. The Pearson correlation between predicted and observed expression was calculated and the P value distribution of the correlation was evaluated using π_1 statistics. We calculated π_1 values in the test populations using several MESA model predictive performance R^2 thresholds for gene inclusion ($R^2 = 0$, 0.01, 0.05, 0.1, and 0.2).

S-PrediXcan application of MESA gene expression prediction models

We performed S-PrediXcan [37] with MESA models AFA, HIS, CAU, AFHI, and ALL using publicly available multiancestry GWAS summary statistics from a large asthma study by the Trans-National Asthma Genetic Consortium (TAGC) [38]. TAGC contained 23,948 cases and 118,538 controls with the following ancestry proportions: 127,669 European, 8,204 African, 5,215 Japanese, and 1,398 Latino [38]. The Bonferroni correction threshold used to define significant genes was calculated as $P < (0.05/\text{gene count})$.

Supporting information

S1 Fig. Genotypic principal component (PC) analysis of MESA populations. PC1 vs. PC2 plots of each MESA population when analyzed with HapMap populations show varying degrees of admixture. The HapMap populations are defined by the following abbreviations: Yoruba from Ibadan, Nigeria (YRI), European ancestry from Utah (CEU), East Asians from Beijing, China and Tokyo, Japan (ASN). (A) MESA AFA population (red), (B) MESA HIS population (green), (C) MESA CAU population (blue), (D) all MESA populations combined. (TIF)

S2 Fig. Consistent cis-eQTL results with 3 or more genotypic principal components (PCs). cis-eQTL count (FDR < 0.05) vs. the number of PEER factors used to adjust for hidden confounders in the expression data of each MESA population. The number of genotypic PCs is listed in the gray title box and the color of the lines represent each MESA population. Note that all curves with at least 3 genotypic PCs look the same. AFA = MESA African American, CAU = MESA European American, HIS = MESA Hispanic American. (TIFF)

S3 Fig. Pairwise cis-eQTL true positive rates across all PEER factor combinantions. True positive rate π_1 statistics [29] for cis-eQTLs are plotted comparing each Discovery Population to each Replication Population. The number after each population abbreviation is the number of PEER factors used to adjust for hidden confounders in the expression data. Higher π_1 values indicate a stronger replication signal. π_1 is calculated when the SNP-gene pair from the discovery population is present in the replication population. All models shown included 3 genotypic principal components. AFA = MESA African American, CAU = MESA European American,

HIS = MESA Hispanic American, FHS = Framingham Heart Study, GEU = Geuvadis,
MXL = Mexicans in Los Angeles, YRI = Yoruba in Ibadan, Nigeria.
(TIFF)

S4 Fig. Higher heritability genes have higher genetic correlation (rG) and lower standard error (SE) estimates between MESA populations. (A) Pairwise population comparison of minimum heritability (h^2) and rG standard error (SE) for each gene. The y-axis is the minimum h^2, the x-axis is the $-log_{10}$ SE of the rG estimate, and the points are colored according to the maximum h^2 between the populations titling each plot. (B) rG compared to $-log_{10}$ SE of the estimate. Genes with low SE are more likely to have a positive rG estimate. (C) Comparison of the genetic correlation between pairwise MESA populations and the subset of genes with normalized h^2 greater than a given threshold in the AFA population. h^2 estimates are normalized by the number of SNPs used in the estimate, i.e. those within 1 Mb of each gene.
(TIFF)

S5 Fig. Comparison of gene expression proportion variance explained (PVE) estimates of models assuming different underlying genetic architectures. (A) Bayesian Sparse Linear Mixed Modeling (BSLMM) includes both sparse and polygenic components and estimates the total percent variance explained (PVE) and the parameter PGE, which represents the proportion of the genetic variance explained by sparse effects. The highly heritable genes (high PVE) have PGE near 1 and therefore the local genetic architecture is sparse. There is not enough evidence to determine if the lower heritablility genes are more sparse or polygenic. (B) The difference between PVE of BSLMM and LMM or BVSR is compared to the BSLMM PVE across genes in MESA populations AFA, HIS, and CAU. (C) Zoomed in plot of B using contour lines from two-dimensional kernel density estimation to visualize where the points are concentrated. For both LMM and BVSR, the PVE difference values (y-axis) are above the horizontal line at zero indicating that both models perform worse than BSLMM. However, the difference between LMM and BSLMM is greater than between BVSR and BSLMM, which indicates sparse effects predominate for most genes.
(TIFF)

S6 Fig. Consistent elastic net results with 10 or more PEER factors. Comparison of the elastic net ($\alpha = 0.5$) cross-validated predictive performance R^2 in models with different numbers of PEER factors as covariates. Across populations, models with 10 PEER factors shows increased predictive performance over 0 PEER factors, while models with 10, 20, or 30 PEER factors perform similarly.
(TIFF)

S7 Fig. Consistent elastic net results with downsampled populations. The CAU and HIS populations were randomly downsampled to include the same sample size as AFA (n = 233). Predictive performance was measured within each population using nested cross-validation. (A) Comparison of the elastic net ($\alpha = 0.5$) predictive performance R^2 of the full sample to the downsampled population. Spearman correlations were 0.81 and 0.83 for CAU and HIS sample comparisons, respectively. (B) Comparison of predictive performance for each gene (R^2) between each pair of populations. In each gray title box, population 1 is listed first and population 2 is listed second. The identity line is shown in blue. The pairwise Spearman correlations (ρ) between genes are AFA-CAU downsample: $\rho = 0.54$, AFA-HIS downsample: $\rho = 0.61$, HIS downsample-CAU downsample: $\rho = 0.65$.
(TIFF)

S8 Fig. Comparison of weighted F$_{ST}$ between gene models with large ($>$ t) and small ($<=$ t) differences in predictive performance R^2. For each gene model, weighted average F$_{ST}$ was calculated by multiplying each beta from the elastic net model by that SNP's F$_{ST}$ before taking the mean across SNPs. The gene groups with the larger absolute value R^2 difference between populations had significantly larger weighted F$_{ST}$ at each difference threshold, t (Wilcoxon rank sum tests, $P < 2.2 \times 10^{-16}$).
(TIFF)

S1 Table. Bonferroni significant S-PrediXcan results using gene expression prediction models from different MESA populations and summary statistics from a multiancestry GWAS of asthma.
(TXT)

S2 Table. All S-PrediXcan results using gene expression prediction models from different MESA populations and summary statistics from a multiancestry GWAS of asthma.
(TXT)

Author Contributions

Conceptualization: Heather E. Wheeler.

Data curation: Lauren S. Mogil, Angela Andaleon, Alexa Badalamenti, Heather E. Wheeler.

Formal analysis: Lauren S. Mogil, Angela Andaleon, Alexa Badalamenti, Xiuqing Guo, Heather E. Wheeler.

Funding acquisition: Jerome I. Rotter, Hae Kyung Im, Yongmei Liu, Heather E. Wheeler.

Investigation: Heather E. Wheeler.

Methodology: Scott P. Dickinson, Heather E. Wheeler.

Project administration: Heather E. Wheeler.

Resources: Xiuqing Guo, Jerome I. Rotter, W. Craig Johnson, Hae Kyung Im, Yongmei Liu, Heather E. Wheeler.

Software: Scott P. Dickinson, Hae Kyung Im, Heather E. Wheeler.

Supervision: Heather E. Wheeler.

Validation: Lauren S. Mogil, Heather E. Wheeler.

Visualization: Lauren S. Mogil, Heather E. Wheeler.

Writing – original draft: Lauren S. Mogil, Heather E. Wheeler.

Writing – review & editing: Lauren S. Mogil, Angela Andaleon, Alexa Badalamenti, Scott P. Dickinson, Xiuqing Guo, Jerome I. Rotter, W. Craig Johnson, Hae Kyung Im, Yongmei Liu, Heather E. Wheeler.

References

1. MacArthur J, Bowler E, Cerezo M, Gil L, Hall P, Hastings E, et al. The new NHGRI-EBI Catalog of published genome-wide association studies (GWAS Catalog). Nucleic acids research. 2017; 45(D1):D896–D901. https://doi.org/10.1093/nar/gkw1133 PMID: 27899670

2. Need AC, Goldstein DB. Next generation disparities in human genomics: concerns and remedies. Trends in Genetics. 2009; 25(11):489–494. https://doi.org/10.1016/j.tig.2009.09.012 PMID: 19836853

3. Bustamante CD, De La Vega FM, Burchard EG. Genomics for the world. Nature. 2011; 475(7355):163–165. https://doi.org/10.1038/475163a PMID: 21753830

4. Popejoy AB, Fullerton SM. Genomics is failing on diversity. Nature. 2016; 538(7624):161–164. https://doi.org/10.1038/538161a PMID: 27734877

5. Martin AR, Gignoux CR, Walters RK, Wojcik GL, Neale BM, Gravel S, et al. Human Demographic History Impacts Genetic Risk Prediction across Diverse Populations. American Journal of Human Genetics. 2017; 100(4):635–649. https://doi.org/10.1016/j.ajhg.2017.03.004 PMID: 28366442

6. Gravel S, Henn BM, Gutenkunst RN, Indap AR, Marth GT, Clark AG, et al. Demographic history and rare allele sharing among human populations. Proceedings of the National Academy of Sciences. 2011; 108(29):11983–11988. https://doi.org/10.1073/pnas.1019276108

7. Carlson CS, Matise TC, North KE, Haiman CA, Fesinmeyer MD, Buyske S, et al. Generalization and Dilution of Association Results from European GWAS in Populations of Non-European Ancestry: The PAGE Study. PLoS Biology. 2013; 11(9). https://doi.org/10.1371/journal.pbio.1001661 PMID: 24068893

8. Oh SS, Galanter J, Thakur N, Pino-Yanes M, Barcelo NE, White MJ, et al. Diversity in Clinical and Biomedical Research: A Promise Yet to Be Fulfilled. PLoS Medicine. 2015; 12(12):e1001918. https://doi.org/10.1371/journal.pmed.1001918 PMID: 26671224

9. Nica AC, Montgomery SB, Dimas AS, Stranger BE, Beazley C, Barroso I, et al. Candidate causal regulatory effects by integration of expression QTLs with complex trait genetic associations. PLoS Genetics. 2010; 6(4):e1000895. https://doi.org/10.1371/journal.pgen.1000895 PMID: 20369022

10. Gusev A, Lee SH, Trynka G, Finucane H, Vilhjálmsson BJ, Xu H, et al. Partitioning heritability of regulatory and cell-type-specific variants across 11 common diseases. American Journal of Human Genetics. 2014; 95(5):535–552. https://doi.org/10.1016/j.ajhg.2014.10.004 PMID: 25439723

11. Torres JM, Gamazon ER, Parra EJ, Below JE, Valladares-Salgado A, Wacher N, et al. Cross-tissue and tissue-specific eQTLs: Partitioning the heritability of a complex trait. American Journal of Human Genetics. 2014; 95(5):521–534. https://doi.org/10.1016/j.ajhg.2014.10.001 PMID: 25439722

12. Davis LK, Yu D, Keenan CL, Gamazon ER, Konkashbaev AI, Derks EM, et al. Partitioning the Heritability of Tourette Syndrome and Obsessive Compulsive Disorder Reveals Differences in Genetic Architecture. PLoS Genetics. 2013; 9(10):e1003864. https://doi.org/10.1371/journal.pgen.1003864 PMID: 24204291

13. Li YI, Van De Geijn B, Raj A, Knowles DA, Petti AA, Golan D, et al. RNA splicing is a primary link between genetic variation and disease. Science. 2016; 352(6285):600–604. https://doi.org/10.1126/science.aad9417 PMID: 27126046

14. Stranger BE, Montgomery SB, Dimas AS, Parts L, Stegle O, Ingle CE, et al. Patterns of Cis regulatory variation in diverse human populations. PLoS Genetics. 2012; 8(4):e1002639. https://doi.org/10.1371/journal.pgen.1002639 PMID: 22532805

15. Battle A, Mostafavi S, Zhu X, Potash JB, Weissman MM, McCormick C, et al. Characterizing the genetic basis of transcriptome diversity through RNA-sequencing of 922 individuals. Genome Research. 2014; 24(1):14–24. https://doi.org/10.1101/gr.155192.113 PMID: 24092820

16. Kelly DE, Hansen MEB, Tishkoff SA. Global variation in gene expression and the value of diverse sampling. Current Opinion in Systems Biology. 2017; 1:102–108. https://doi.org/10.1016/j.coisb.2016.12.018 PMID: 28596996

17. Aguet F, Brown AA, Castel SE, Davis JR, He Y, Jo B, et al. Genetic effects on gene expression across human tissues. Nature. 2017; 550(7675):204–213. https://doi.org/10.1038/nature24277

18. Wheeler HE, Shah KP, Brenner J, Garcia T, Aquino-Michaels K, Cox NJ, et al. Survey of the Heritability and Sparse Architecture of Gene Expression Traits across Human Tissues. PLoS Genetics. 2016; 12(11):e1006423. https://doi.org/10.1371/journal.pgen.1006423 PMID: 27835642

19. Manor O, Segal E. Robust Prediction of Expression Differences among Human Individuals Using Only Genotype Information. PLoS Genetics. 2013; 9(3):e1003396. https://doi.org/10.1371/journal.pgen.1003396 PMID: 23555302

20. Gamazon ER, Wheeler HE, Shah KP, Mozaffari SV, Aquino-Michaels K, Carroll RJ, et al. A gene-based association method for mapping traits using reference transcriptome data. Nature Genetics. 2015; 47(9):1091–1098. https://doi.org/10.1038/ng.3367 PMID: 26258848

21. Gusev A, Ko A, Shi H, Bhatia G, Chung W, Penninx BWJH, et al. Integrative approaches for large-scale transcriptome-wide association studies. Nature Genetics. 2016; 48(3):245–252. https://doi.org/10.1038/ng.3506 PMID: 26854917

22. Albert FW, Kruglyak L. The role of regulatory variation in complex traits and disease. Nature Reviews Genetics. 2015; 16(4):197–212. https://doi.org/10.1038/nrg3891 PMID: 25707927

23. Sajuthi SP, Sharma NK, Chou JW, Palmer ND, McWilliams DR, Beal J, et al. Mapping adipose and muscle tissue expression quantitative trait loci in African Americans to identify genes for type 2 diabetes and obesity. Human Genetics. 2016; 135(8):869–880. https://doi.org/10.1007/s00439-016-1680-8 PMID: 27193597

24. Bild DE, Bluemke DA, Burke GL, Detrano R, Diez Roux AV, Folsom AR, et al. Multi-Ethnic Study of Atherosclerosis: Objectives and design. American Journal of Epidemiology. 2002; 156(9):871–881. https://doi.org/10.1093/aje/kwf113 PMID: 12397006

25. Liu Y, Ding J, Reynolds LM, Lohman K, Register TC, De la Fuente A, et al. Methylomics of gene expression in human monocytes. Human Molecular Genetics. 2013; 22(24):5065–5074. https://doi.org/10.1093/hmg/ddt356 PMID: 23900078

26. Lappalainen T, Sammeth M, Friedländer MR, 'T Hoen PAC, Monlong J, Rivas MA, et al. Transcriptome and genome sequencing uncovers functional variation in humans. Nature. 2013; 501(7468):506–511. https://doi.org/10.1038/nature12531 PMID: 24037378

27. Zhang X, Joehanes R, Chen BH, Huan T, Ying S, Munson PJ, et al. Identification of common genetic variants controlling transcript isoform variation in human whole blood. Nature Genetics. 2015; 47(4):345–352. https://doi.org/10.1038/ng.3220 PMID: 25685889

28. Stegle O, Parts L, Piipari M, Winn J, Durbin R. Using probabilistic estimation of expression residuals (PEER) to obtain increased power and interpretability of gene expression analyses. Nature Protocols. 2012; 7(3):500–507. https://doi.org/10.1038/nprot.2011.457 PMID: 22343431

29. Storey JD, Tibshirani R. Statistical significance for genomewide studies. Proceedings of the National Academy of Sciences. 2003; 100(16):9440–9445. https://doi.org/10.1073/pnas.1530509100

30. Yang J, Lee SH, Goddard ME, Visscher PM. GCTA: A tool for genome-wide complex trait analysis. American Journal of Human Genetics. 2011; 88(1):76–82. https://doi.org/10.1016/j.ajhg.2010.11.011 PMID: 21167468

31. Lee SH, Yang J, Goddard ME, Visscher PM, Wray NR. Estimation of pleiotropy between complex diseases using single-nucleotide polymorphism-derived genomic relationships and restricted maximum likelihood. Bioinformatics. 2012; 28(19):2540–2542. https://doi.org/10.1093/bioinformatics/bts474 PMID: 22843982

32. Brown BC, Ye CJ, Price AL, Zaitlen N. Transethnic Genetic-Correlation Estimates from Summary Statistics. American Journal of Human Genetics. 2016; 99(1):76–88. https://doi.org/10.1016/j.ajhg.2016.05.001 PMID: 27321947

33. Friedman J, Hastie T, Tibshirani R. Regularization Paths for Generalized Linear Models via Coordinate Descent. Journal of Statistical Software. 2010; 33(1):1–22. https://doi.org/10.18637/jss.v033.i01 PMID: 20808728

34. Tibshirani R. Regression shrinkage and selection via the lasso: A retrospective. Journal of the Royal Statistical Society Series B: Statistical Methodology. 2011; 73(3):273–282. https://doi.org/10.1111/j.1467-9868.2011.00771.x

35. Zhou X, Carbonetto P, Stephens M. Polygeneic modeling with {B}ayesian sparse linear mixed models. PLoS Genet. 2013; 9(2):e1003264. https://doi.org/10.1371/journal.pgen.1003264 PMID: 23408905

36. Guan Y, Stephens M. Bayesian variable selection regression for genome-wide association studies and other large-scale problems. Annals of Applied Statistics. 2011; 5(3):1780–1815. https://doi.org/10.1214/11-AOAS455

37. Barbeira AN, Dickinson SP, Bonazzola R, Zheng J, Wheeler HE, Torres JM, et al. Exploring the phenotypic consequences of tissue specific gene expression variation inferred from GWAS summary statistics. Nature Communications. 2018; 9(1):1825. https://doi.org/10.1038/s41467-018-03621-1 PMID: 29739930

38. Demenais F, Margaritte-Jeannin P, Barnes KC, Cookson WOC, Altmüller J, Ang W, et al. Multiancestry association study identifies new asthma risk loci that colocalize with immune-cell enhancer marks. Nature Genetics. 2018; 50(1):42–53. https://doi.org/10.1038/s41588-017-0014-7 PMID: 29273806

39. Fritsche LG, Igl W, Bailey JNC, Grassmann F, Sengupta S, Bragg-Gresham JL, et al. A large genome-wide association study of age-related macular degeneration highlights contributions of rare and common variants. Nature Genetics. 2015; 48(2):134–143. https://doi.org/10.1038/ng.3448 PMID: 26691988

40. Zhu Z, Zhang F, Hu H, Bakshi A, Robinson MR, Powell JE, et al. Integration of summary data from GWAS and eQTL studies predicts complex trait gene targets. Nature Genetics. 2016; 48(5):481–487. https://doi.org/10.1038/ng.3538 PMID: 27019110

41. Zeng P, Zhou X. Non-parametric genetic prediction of complex traits with latent Dirichlet process regression models. Nature Communications. 2017; 8(1). https://doi.org/10.1038/s41467-017-00470-2

42.   Gottlieb A, Daneshjou R, DeGorter M, Bourgeois S, Svensson PJ, Wadelius M, et al. Cohort-specific imputation of gene expression improves prediction of warfarin dose for African Americans. Genome Medicine. 2017; 9(1). https://doi.org/10.1186/s13073-017-0495-0 PMID: 29178968

43.   Pickrell JK, Berisa T, Liu JZ, Ségurel L, Tung JY, Hinds DA. Detection and interpretation of shared genetic influences on 42 human traits. Nature Genetics. 2016; 48(7):709–717. https://doi.org/10.1038/ng.3570 PMID: 27182965

44.   Auton A, Abecasis GR, Altshuler DM, Durbin RM, Abecasis GR, Bentley DR, et al. A global reference for human genetic variation. Nature. 2015; 526(7571):68–74. https://doi.org/10.1038/nature15393 PMID: 26432245

45.   Das S, Forer L, Schönherr S, Sidore C, Locke AE, Kwong A, et al. Next-generation genotype imputation service and methods. Nature Genetics. 2016; 48(10):1284–1287. https://doi.org/10.1038/ng.3656 PMID: 27571263

46.   Loh PR, Danecek P, Palamara PF, Fuchsberger C, Reshef YA, Finucane HK, et al. Reference-based phasing using the Haplotype Reference Consortium panel. Nature Genetics. 2016; 48(11):1443–1448. https://doi.org/10.1038/ng.3679 PMID: 27694958

47.   Price AL, Patterson NJ, Plenge RM, Weinblatt ME, Shadick NA, Reich D. Principal components analysis corrects for stratification in genome-wide association studies. Nature Genetics. 2006; 38(8):904–909. https://doi.org/10.1038/ng1847 PMID: 16862161

48.   Shabalin AA. Matrix eQTL: ultra fast eQTL analysis via large matrix operations. Bioinformatics. 2012; 28(10):1353–1358. https://doi.org/10.1093/bioinformatics/bts163 PMID: 22492648

49.   Zhou X, Stephens M. Genome-wide efficient mixed-model analysis for association studies. Nature Genetics. 2012; 44(7):821–824. https://doi.org/10.1038/ng.2310 PMID: 22706312

50.   Weir BS, Cockerham CC. Estimating F-statistics for the analysis of population structure. Evolution. 1984; 38(6):1358–1370. https://doi.org/10.1111/j.1558-5646.1984.tb05657.x PMID: 28563791